Synthesis and characterization of silver, gold, copper oxide and titanium dioxide sponges using Triton X-305 as sacrificial hydrogel template

Farid Khan* and Ruchi Bilgainya

Nanomaterials Discovery Laboratory, Department of Chemistry, Dr H. S. Gour Central University, Sagar 470 003, India

A novel approach is presented to synthesize silver (Ag), gold (Au), copper oxide (CuO) and titanium dioxide (TiO_2) sponges by template sacrifice route using Triton X-305 as the sacrificial template. Scanning electron microscopy, X-ray diffraction, thermogravimetric analysis and Brunauer–Emmett–Teller adsorption isotherm techniques were used to characterize the monoliths. Additives like dextran, silica nanoparticles and 1,3,5-trimethylbenzene significantly affect the pore sizes of the monoliths. The pore size of the monoliths varied from 50 nm to 7 μm. The surface areas of porous Ag, Au, CuO and TiO_2 reported were always higher than their simple metals.

Keywords: Metal oxide sponges, porous materials, sol–gel method, template sacrifice route.

POROUS scaffolds have unique properties such as good thermal conductivity, gas permeability, low density, useful mechanical and chemical properties, bio-filtration capability and high surface area. Therefore such materials are extensively used in molecular catalysis, photonic crystals, biosensor technology, tissue engineering, targeted drug delivery, heat dissipation, fuel cell technology and nanoreactors[1–4]. Colloidal crystal templating, de-alloying, electrochemical deposition, organic polymerization and sol–gel followed by template sacrifice route method are used to synthesize porous metal and metal oxide sponges[5–8]. But the latter uses acid or base as catalyst, which is toxic. Significant work has been done by Mann and co-workers[9] on macroporous framework of silver (Ag), gold (Au) and copper oxide (CuO) using dextran as template. However, the Ag monolith has a surface area of 0.5 m^2/g. Khan *et al.*[10] have reported the macroporous sponges of Ag with surface area around 2 m^2/g by calcining Ag/Triton X-114 composite. Surface area of macroporous Au prepared by the calcination of Au/Triton X-165/dextran xerogel was found to be 8.26 m^2/g (ref. 11). Mesoporous Au sponge with pore size of 15 nm has been synthesized[12] by de-alloying of $AuAl_2$ with NaOH. The less noble metal (Ag) dissolves from a binary alloy, whereas the more noble metal (Au) self-organizes an open-cell structure. Pores are formed by the aggregation of chemically driven noble atoms into two-dimensional clusters by phase separation[13]. Mesoporous, crystalline, titanium dioxide (TiO_2) macrocellular foams were synthesized using Pluronic (P_{123}) as surfactant[14]. Several mesoporous transition-metal oxides have been synthesized, including TiO_2, ZrO_2, Nb_2O_5, WO_3, MnO_x, V_2O_3, CrO_x, Fe_2O_3 and Co_3O_4, although mesoporous copper oxides are of particular interest[15,16]. Facile, environmentally friendly fabrication of macroporous Ag frameworks has been made using the ionic liquid N-(2-hydroxyethyl)-ammonium formate[17]. Ag-doped mesoporous TiO_2 framework was reported by Engelhard *et al.*[18] by non-ionic surfactants like Pluronic F_{127}. Supercritical drying technique was also used to synthesize TiO_2 mesoporous materials using liquid CO_2. The materials showed good photocatalytic activity[19,20]. Here we report the porous Ag, Au, CuO and TiO_2 sponges using Triton X-305 as hydrogel template utilizing the sol–gel method without the use of acid or base.

Ag monoliths were prepared by dissolving 2.4 g $AgNO_3$ (BDH) in 2 g of distilled water and 2.4 g Triton X-305 (Fluka) was added at room temperature. The gel was stirred for 10 min to form a paste, which gradually became dark in colour. The resulting gel was aged for 60 h at room temperature and then calcined at 600°C for 2 h followed by cooling to room temperature. The rate of heating and cooling was 2°C/min, which was controlled using a Carbolite EFI furnace.

Ag/Triton X-305/dextran ($Mw = 2 \times 10^6$, Fluka), Ag/Triton X-305/ludox (As-40, colloidal silica, 40 wt% suspension in water, Sigma–Aldrich) and Ag/Triton X-305/TMB (Fluka) monoliths were prepared using the above protocol by adding 2.5 g dextran in 5 g water, 0.21 g ludox or 3.02 g 1,3,5 trimethyl benzene (TMB) separately to Ag/Triton X-305 gel. The dextran and TMB-containing gels were calcined at 600°C with the above heating and cooling rates, whereas the Ag/Triton X-305/ludox gel was calcined at 800°C for 1 h with heating and cooling rates of 2°C/min. The calcined ludox monolith was treated with 30% HF (Sigma–Aldrich) for 34 h, followed by washing with water several times to remove silica from the monolith.

Au/Triton X-305/dextran frameworks were prepared by dissolving 2 g $AuCl_3$ (99.99%; Sigma–Aldrich) in 30 g water and adding 5.17 g Triton X-305, followed by the addition of a paste of dextran prepared by dissolving 16 g dextran in 4 g water, and stirring for 15 min. The resulting yellow viscous gel was aged for 20 days to allow polysaccharide-mediated reduction of the Au (III) complex to metallic Au. The resulting gel was calcined at 800°C for 2 h at a heating rate 5°C/min, followed by cooling at the rate of 5°C/min to room temperature.

CuO monoliths, 4 g copper (II) nitrate pentahemihydrate (Riedel-deHaen), were dissolved in 4 g water and 2 g Triton X-305, and a paste of dextran was prepared by dissolving 2 g in 2 g water added. The resulting gel was stirred using a magnetic stirrer for 30 min at 50°C to

*For correspondence. (e-mail: faridkhan58@yahoo.com)

Table 1. Surface areas of monoliths

Monolith	Pore size (μm)	X-ray diffraction (face)	Surface area ($m^2 g^{-1}$)
Ag/Triton X-305	1–2	Face-centred cubic lattice	3.68
Ag/Triton X-305/dextran	1–5	Face-centred cubic lattice	6.45
Ag/Triton X-305/ludox	0.3–5	Face-centred cubic lattice	9.01
Ag/Triton X-305/TMB	1.5–6	Face-centred cubic lattice	2.36
Au/Triton X-305/dextran	0.5–7	Face-centred cubic lattice	9.89
CuO/Triton X-305/dextran	0.1–0.15	Tenorite (with bcc)	27.35
TiO_2/Triton X-305/dextran	0.05–0.25	Rutile	36.32

Figure 1. Silver monoliths after calcination. ***a***, Ag sponge after calcination of Ag/Triton X-305 xerogel. ***b***, Ag monolith after calcination of Ag/Triton X-305/dextran xerogel. ***c***, Ag framework after calcination of Ag/Triton X-305/TMB xerogel.

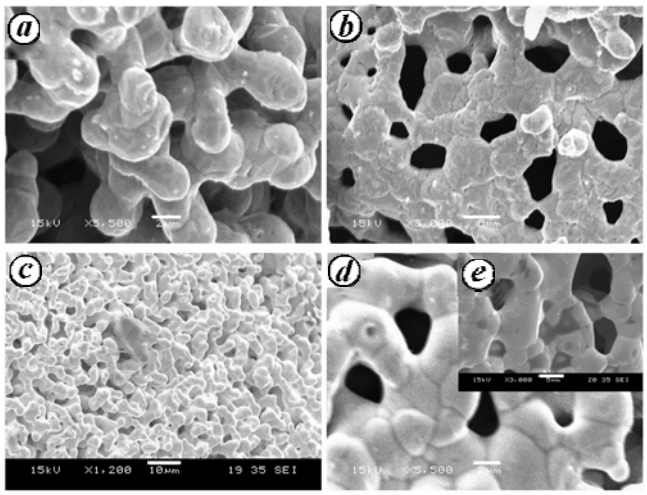

Figure 2. Scanning electron microscopic (SEM) images of Ag macroporous sponges using Triton X-305 gel as sacrificial template. Monoliths prepared by calcination of: ***a***, Ag/Triton X-305 gel showing pores of 1–2 μm in size, scale bar 2 μm; ***b***, Ag/Triton X-305/dextran gel with pore size varying from 1 to 5 μm, scale bar 5 μm; ***c***, Ag/Triton X-305/ludox gel after HF treatment showing pore size varying from 300 nm to 5 μm, scale bar = 10 μm; ***d***, ***e***, Ag/Triton X-305/TMB gel with pore size varying from 1.5 to 8 μm, scale bar 2 and 5 μm respectively. Ag nanoparticles of size 100–400 nm were observed in the monoliths (***a***–***e***).

produce a blue-green gel that was aged for 4 days at room temperature. Then the gel was calcined at 600°C for 2 h at a heating and cooling rate of 5°/min.

Ti/Triton X-305/dextran gel was prepared by adding 8 g Triton X-305 (Sigma–Aldrich) to 8 g titanium (IV) isopropoxide (Sigma–Aldrich, Mw = 284.26) in a beaker and stirred well for 5 min. Then a paste of dextran prepared by dissolving 8 g dextran ($Mw = 2 \times 10^6$) in 20 g water was added and, the resulting gel was stirred again for 10 min. The gel was aged for 3 days at room temperature and calcined at 850°C at the heating and cooling rate of 2°/min.

Scanning electron microscopic (SEM) study was performed on a JEOL 5600 microscope. Except CuO and TiO_2 monoliths, which were coated with Pt and Pd, the other monoliths were coated with carbon and placed on aluminium stubs to get the SEM images.

Powder X-ray diffraction (PXRD) patterns were recorded on a Brucker D8 diffractometer using Cu-Kα radiation. Thermogravimetric analysis (TGA) profiles were obtained using a NETZSCH Simultaneous Thermal Analyser (STA 409 EP) with alumina reference crucible.

The Brunauer, Emmitt and Teller (BET) surface areas of Ag, Au, CuO and TiO_2 monoliths prepared from Triton X-305 using different additives are given in Table 1. Quantachrome Autosorb-1C instrument was used to measure the surface area at –196°C. The corresponding micropore size distribution was determined from the BJH model using the desorption branch isotherms.

After calcination, white monoliths of porous Ag (Figure 1) were obtained. Figure 2 *a* shows the SEM images of self-supporting scaffold of Ag prepared using Triton X-305 with a disordered network of pores varying from 1 to 2 μm. Pore sizes between 1 and 5 μm were observed when dextran was added to the Ag/Triton X-305 gel (Figure 2 *b*) whereas in the case of Ag/Triton X-305/ludox (HF) treatment, there were significantly smaller pores with size ranging from 0.3 to 5 μm (Figure 2 *c*). HF-treated monoliths showed the absence of silica nanoparticles by EDAX analysis (figure not shown). Addition of TMB as a swelling agent to Ag/Triton X-305 gels produced slightly bigger pores, with size varying from 1.5 to 6 μm (Figure 2 *d*). TMB acts as a swelling agent to enlarge the pore size because it is a nonpolar compound which solubilizes inside the surfactant assembly, thus increasing the volume of the resulting composite.

Similar experiments using Triton X-305 gels containing $AuCl_3$ or titanium (IV) isopropoxide, or copper (II) nitrate produced intact macroporous monoliths, which were yellow, white and black respectively. SEM studies indicated pore sizes from 500 nm to 7 μm in Au/Triton X-305/dextran monoliths (Figure 3 *a*) and 50 to 250 nm in Ti/Triton X-305/dextran monoliths (Figure 3 *b*) respectively. Significant smaller pores with size varying from

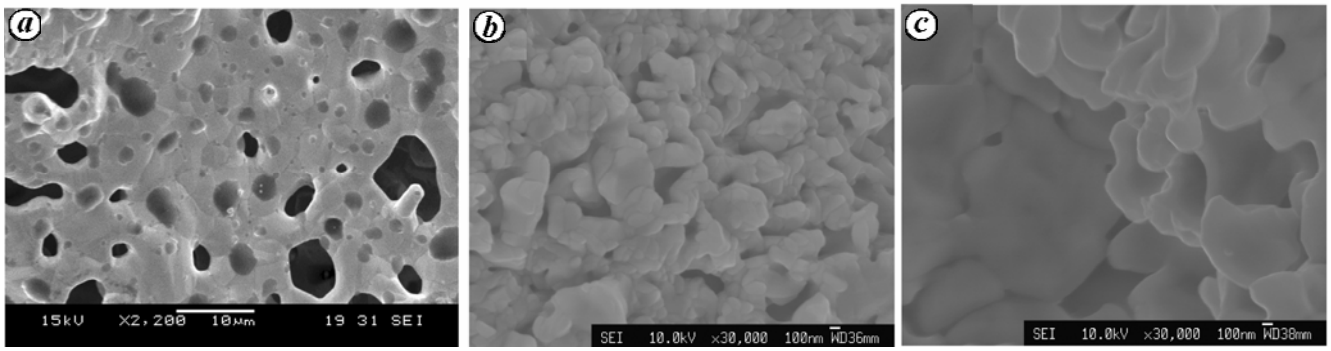

Figure 3. SEM images of Au, TiO_2 and CuO monoliths using Triton X-305 as sacrificial template. ***a***, Au monolith prepared by calcination of Au/Triton X-305/dextran xerogel with pore size varying from 500 nm to 7 µm; scale bar 10 µm. ***b***, TiO_2 monolith showing pore sizes of 50–250 nm prepared by calcination of a TiO_2/Triton X-305/dextran xerogel; scale bar 100 nm. ***c***, CuO monolith with pore size varying from 100 to 150 nm, synthesized by calcination of copper nitrate/Triton X-305/dextran xerogel; scale bar 100 nm.

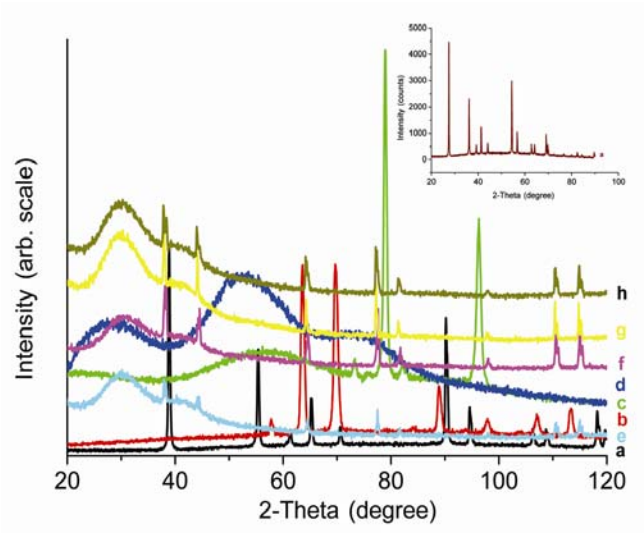

Figure 4. X-ray diffraction (XRD) patterns of titanium dioxide (TiO_2), silver (Ag), gold (Au) and copper oxide (CuO) monoliths with Triton X-305 as templates. (a) TiO_2/Triton X-305/dextran monolith. (b) CuO/Triton X-305/dextran framework. (c) Au/Triton X-305/dextran monolith. (d) Sample holder (poly(methyl) methacrylate, PMMA). (e–h) Ag monoliths: (e) Ag/Triton X-305, (f) Ag/Triton X-305/dextran; (g) Ag/Triton X-305/ludox (after HF treatment), and (h) Ag/Triton X-305/TMB. TiO_2 showed reflections at *d* spacings of 3.24, 2.49, 2.31, 2.19, 2.05, 1.68, 1.62, 1.47, 1.45, 1.36, 1.34, 1.24 and 1.16 Å, which correspond to (110), (101), (200), (111), (210), (211), (220), (002), (310), (301), (112), (202) and (321) lattice planes of a rutile lattice tetragonal unit cell (JCPDS (Joint Committee on Power Diffraction Standard) card 4.783. (Inset) Original XRD plot of TiO_2 monolith). CuO monolith showed reflections at 2.74, 2.51, 2.30, 1.86, 1.70, 1.58, 1.50, 1.41, 1.40, 1.37, 1.30, 1.26 and 1.16 Å, which correspond to (110), (002), (200), (–202), (020), (202), (–113), (022), (–311), (220), (311), (004) and (312) of a base-centred monoclinic unit cell (tenorite). Au monoliths showed reflections at 2.36, 2.04, 1.44, 1.23 and 1.17 Å, corresponding to (111), (200), (220), (311) and (222) lattice planes of a face-centred cubic (FCC) unit cell (original XRD pattern contains all the peaks). Peaks at 3.016, 2.50 and 2.31 Å were also observed indicating the presence of crystalline $AuCl_3$. This phase is the starting material, and could be formed by thermally induced reactions ($AuCl_3$ = $AuCl + Cl_2$ and $3AuCl = AuCl_3 + 2Au$) during monolith preparation. Sample holder (PMMA) showed reflections at 5.15, 2.20 and 2.98 Å, which were observed in case of Ag and Au. Ag monoliths showed reflections at *d* spacings of 2.37, 2.06, 1.45, 1.23, 1.18, 1.02, 0.94 and 0.91 Å, which correspond to {111}, {200}, {220}, {311}, {222}, {400}, {333} and {420} lattice planes of a FCC unit cell.

100 to 150 nm were observed in CuO/Triton X-305/dextran monoliths (Figure 3 *c*), which were black in colour. The colour of the Au monolith was yellow.

XRD studies of TiO_2 monoliths showed reflection of TiO_2 rutile, which confirmed the tetragonal structure (Figure 4 *a*). CuO or Au monoliths, tenorite with a base-centred cubic or face-centred cubic (FCC) unit cell structure were formed (Figure 4 *b* and *c*). Ag monoliths showed reflections pertaining to metallic Ag with a FCC structure (Figure 4 *e–h*). For Ag and Au monoliths, poly (methyl) methacrylate (PMMA) sample holders were used, which showed reflections at 5.13, 2.98 and 2.20 (Figure 4 *d*).

Thermogravimetric analysis curves of Ag xerogels is given in Figures 5 *a–d*. Initially, Ag/Triton X-305 xerogel showed a weight loss of 2% from room temperature to 175°C due to the removal of moisture. Thereafter 40% weight loss was observed as a result of the removal of excess Triton X-305 from it in the temperature range 175–190°C. At 190–270°C, $AgNO_3$ and Triton X-305 were decomposed with 10% loss of weight. $AgNO_3$ decomposed to give Ag metal with a release of considerable O_2 [$Ag(NO_3) = 2Ag + 2NO_2 + O_2$] that promotes the combustion of Triton X-305. O_2 also burnt carbon at lower temperature in the range 270–350°C with 6% weight loss. In the end, 42% Ag was left in the monolith. O_2 released due to the thermal decomposition of $AgNO_3$ also helped burn dextran or TMB with the removal of Triton X-305 in the temperature range 120–300°C, with loss of weight around 55–65%. In the case of Ag/Triton X-305/ludox framework, 60% weight loss was observed in the temperature range 150–180°C due to the removal of excess Triton X-305. Then $AgNO_3$ and Triton X-305 were decomposed in the temperature range 180–360°C with 6% weight loss. C was oxidized to CO_2 between 360°C and 600°C. The final Ag/silica monolith constituted 25% of the initial mass.

Au/Triton X-305/dextran xerogel showed 4% weight loss initially due to the removal of moisture, from room

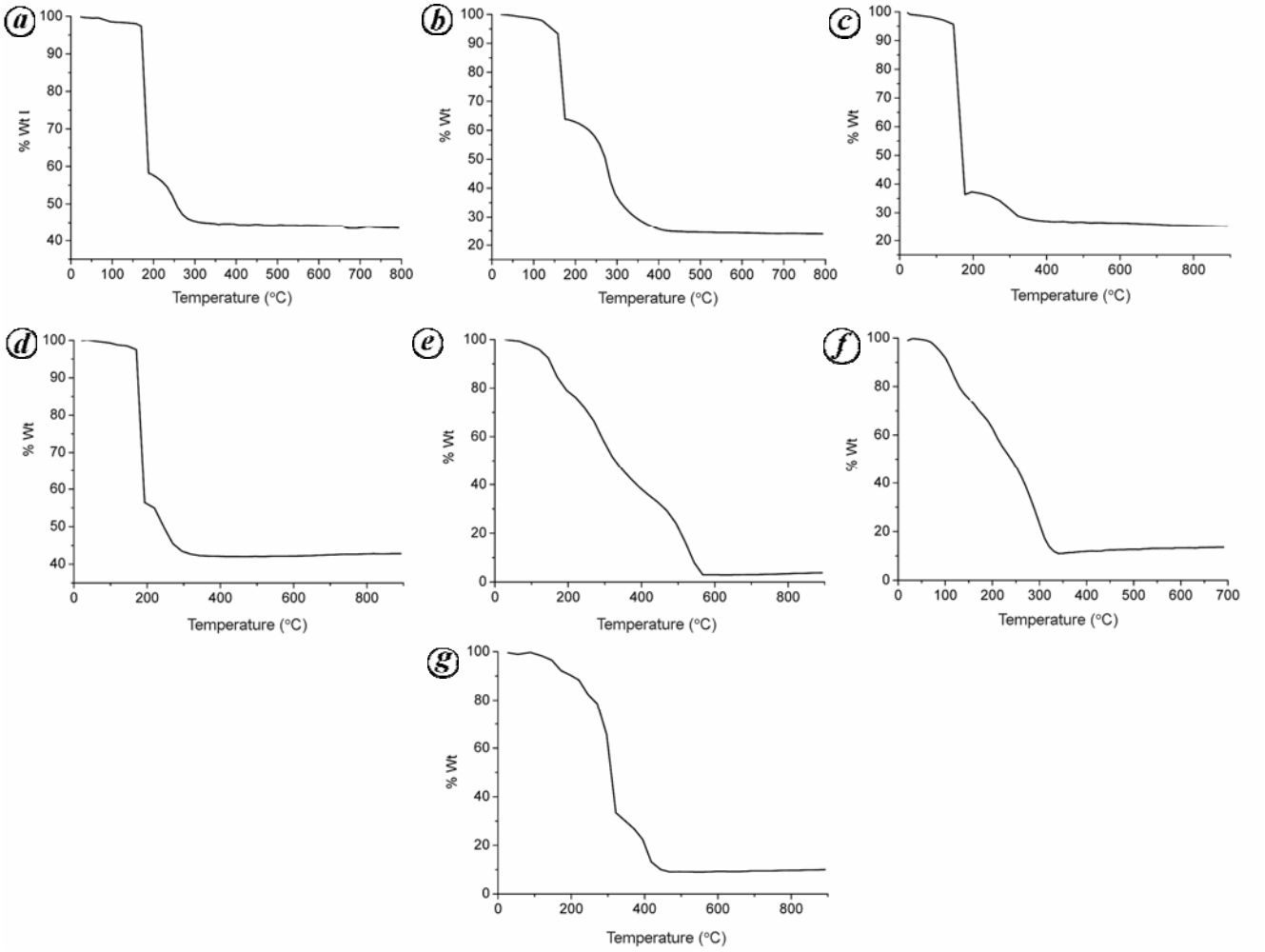

Figure 5. Thermogravimetric analysis graphs for various xerogels: ***a***, Ag/Triton X-305; ***b***, Ag/Triton X-305/dextran; ***c***, Ag/Triton X-305/ludox; ***d***, Ag/Triton X-305/TMB; ***e***, Au/Triton X-305/dextran; ***f***, Copper nitrate/Triton X-305/dextran, and ***g***, TiO_2/Triton X-305/dextran.

temperature to 120°C. Excess Triton X-305 was removed between 120°C and 200°C with 16% weight loss. Then about 55% weight was lost in the temperature range 200–420°C due to the removal of Triton X-305 along with dextran followed by $AuCl_3$, which was converted into AuCl ($AuCl_3 = AuCl + Cl_2$). Thereafter, AuCl decomposed to $AuCl_3$ and Au at 420°C (Figure 5 *e*). Carbon was removed beyond 550°C. Finally, 1% Au with $AuCl_3$ was left in the monolith. In the decomposition of Au/Triton X-305/dextran monolith, O_2 was not released so that Triton X-305 and dextran were decomposed at much higher temperatures.

In CuO/Triton X-305/dextran xerogel (Figure 5 *f*), major weight loss of about 90% was observed between 160°C and 340°C because of the decomposition of Triton X-305 and dextran. In this temperature range, copper nitrate decomposed to CuO with release of NO_2 and O_2 [$Cu(NO_3)_2 = 2CuO + 4NO_2 + O_2$]. This oxygen promoted the decomposition of Triton X-305 and dextran at lower temperature. Carbon was also removed at lower temperature at 350°C. Finally, 10% CuO was left in the monolith.

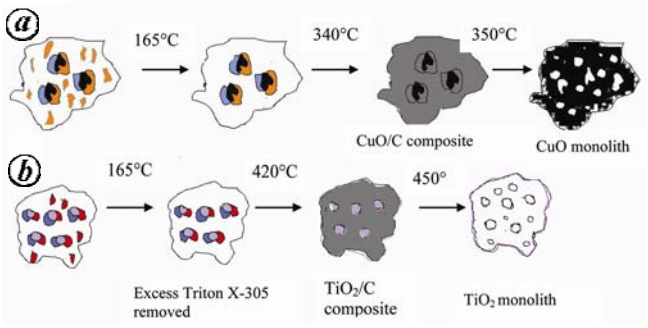

Figure 6. Morphological transformations of CuO and TiO_2 monoliths. ***a***, CuO/Triton X-305/dextran. ***b***, TiO_2/Triton X-305/dextran. Black colour, CuO; red, Triton X-305; blue, dextran; grey, carbon and violet/white, TiO_2.

In the case of Ti/Triton X-305/dextran xerogel (Figure 5 *g*), 2% weight loss was observed due to the removal of moisture present in the monolith. Then in the temperature range 90–420°C, Triton X-305 and dextran were removed with considerable weight loss of about 85%. Carbon was

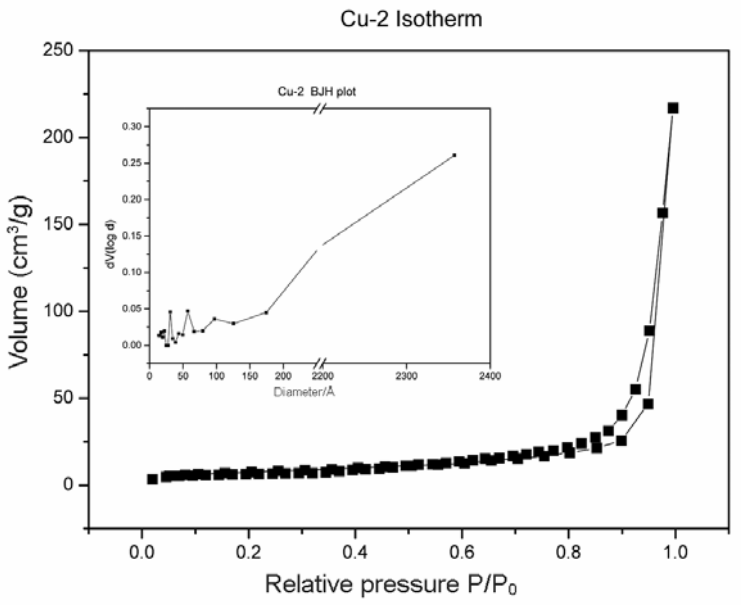

Figure 7. The Brunauer, Emmitt and Teller N_2 adsorption isotherm plots for CuO monolith prepared by the calcination of copper nitrate/Triton X-305/dextran xerogel. (Inset) Micropore size distribution.

removed after 420°C. Finally, 6% TiO_2 was left in the monolith. The morphological changes of CuO and TiO_2 monoliths are given in Figure 6 *a* and *b*.

The BET surface areas of Ag, Au, CuO and TiO_2 monoliths with Triton X-305 as the non-ionic surfactant are given in Table 1. The BET plot between relative pressure (P/P_0) and volume (cm^3/g) for CuO/Triton X-305/dextran monolith is given in Figure 7. The pore size distribution is consistent with the pore size observed by SEM. Generally, the surface area of monoliths depends on calcined temperature; higher the temperature, lesser is the surface area because, at high temperature, the monoliths sinter due to increase in nucleation and densification[21].

It is clear from the present study that using appropriate reaction precursors, porous monoliths of Ag, Au, TiO_2 and CuO can be prepared by thermal decomposition of Triton X-305 hydrogels. Imprinting of micropores on the monoliths depends on controlled outgassing of CO_2 bubbles into the viscous surfactant matrix, such that consolidation of the inorganic reaction products within interstices of the transient foam produces a continuous and interconnected scaffold, rather than localized fragmentation. Pore size increased when dextran or TMB was added to Ag/Triton X-305 hydrogels. We attribute this to changes in the viscosity of the composite gels and their rate of decomposition or solubilization of nonpolar TMB inside the surfactant assembly. However, the addition of silica nanoparticles to the gels reduced the pore size of these monoliths, which suggests that other nanoparticles could also be used to fabricate the monoliths of desired architecture.

Nanoporosity depends on the composition of the hydrogels and also on the nature of the chemical reactions and crystal chemistry of the reaction products. For example, Ag and CuO monoliths can be prepared at lower temperature than Au and TiO_2 monoliths by thermal decomposition of their suitable metal precursors. This is because considerable O_2 was released during chemical reactions which helps to burn their reaction products at lower temperature, whereas in the case of Au and TiO_2, O_2 was not released during calcination. Therefore very high temperature is required for the decomposition of their metal precursors.

We have successfully exploited this noble method to synthesize macroporous monoliths of Ag, Au, CuO and TiO_2 using Triton X-305 as hydrogel template in which no acid or base is used. Significant values of surface areas of these sponges make them technologically more important. In addition, the method is safe, economic and environmentally benign to architect the monoliths for diverse applications[22–25].

1. Zhang, H. and Cooper, A. I., Synthesis and applications of emulsion-templated porous materials. *Soft Matter*, 2005, **1**, 107–113.
2. Velev, O. D. and Kaler, E. W., Structured porous materials via colloidal crystal templating from inorganic oxide to metals. *Adv. Mater*., 2000, **12**, 531–534.
3. Barton, T. J. *et al*., Tailored porous materials. *Chem. Mater*., 1999, **11**, 2633–2656.
4. Studart, A. R., Gonzenbach, U. T., Tervoort, E. and Gauckler, L. J., Processing routes to macroporous ceramics: a review. *J. Am. Ceram. Soc*., 2006, **89**, 1771–1789.
5. Erlebacher, J., Aziz, M. J., Karma, A., Dimitrov, N. and Sieradzki, K., Evolution of nanoporosity in dealloying. *Nature*, 2001, **410**, 450–453.
6. Velev, O. D. and Kaler, E. W., Structured porous materials via colloidal crystal templating from inorganic oxides to metal. *Adv. Mater*., 2000, **12**, 531–534.

7. Kulinowski, K. M., Jiang, P., Vaswani, H. and Colvin, V. L., Porous metals from colloidal templates. *Adv. Mater*., 2000, **12**, 833–837.
8. Zhang, H. and Cooper, A. I., New approaches to synthesis of macroporous metals. *J. Mater. Chem.*, 2005, **15**, 2157–2159.
9. Walsh, D., Arcelli, L., Ikoma, T., Tanaka, S. and Mann, S., Dextran templating for the synthesis of metallic and metal oxide sponges. *Nature Mater*., 2003, **2**, 386–390.
10. Khan, F., Eswaramoorthy, M. and Rao, C. N. R., Macroporous silver monoliths using a simple surfactant. *Solid State Sci*., 2007, **9**, 27–31.
11. Khan, F. and Bilgainya, R., Synthesis and characterization of metal and metal oxide sponges using Triton X-165 as sacrificial template. *Indian J. Chem. A*, 2011, **50**, 55–59.
12. Velev, O. D. and Kaler, E. W., Structured porous materials via colloidal crystal templating from inorganic oxide to metals. *Adv. Mater*., 2000, **12**, 531–534.
13. Erlebacher, J., Aziz, M. J., Karma, A., Dimitrov, N. and Sieradzki, K., Evolution of nanoporosity in dealloying. *Nature*, 2001, **410**, 450–453.
14. Carn, F., Achard, M. F., Bebot, O., Deleuze, H., Reculusa, S. and Backov, R., Synthesis and characterization of highly mesoporous crystalline TiO_2 macrocellular foams. *J. Mater. Chem*., 2005, **15**, 3887–3895.
15. Lai, X., Li, X., Geng, W., Tu, J., Li, J. and Qui, S., Ordered mesoporous copper oxide with crystalline walls. *Angew. Chem., Int. Ed. Engl.*, 2007, **46**, 738–741.
16. Jiao, F., Jumas, J. C., Womes, M., Chadwick, A. V., Harrison, A. and Bruce, P. G., Synthesis of ordered Fe_2O_4 and γ-Fe_2O_3 with crystalline walls using post-templated reduction/oxidation. *J. Am. Chem. Soc*., 2006, **128**, 5468–5474.
17. Richter, K., Backer, T. and Mudring, A. V., Facile environmentally friendly fabrication of porous silver monoliths using the ionic liquid N-(2-hydroxyethyl) ammonium formate. *Chem. Commun*., 2009, 301–303.
18. Li, X. S., Fryxell, G. E., Wang, C. M. and Engelhard, M. H., The synthesis of Ag-doped mesoporous TiO_2. *Micropor. Mesopor. Mater.*, 2008, **111**, 639–642.
19. Horikawa, T., Katoh, M. and Tomida, T., Preparation and characterization of mesoporous titania with high specific surface area. *Micropor. Mesopor. Mater*., 2008, **110**, 397–404.
20. Liu, Y., Wang, M., Li, H., Liu, H., He, P., Yang, X. and Li, J., Preparation and properties of nanostructure anatase TiO_2 monoliths using 1-butyl-3-methyllimidazolium tetrafluoroborate room-temperature ionic liquids as template solvents. *Cryst. Growth Des*., 2005, **5**, 1643–1649.
21. Han, Y. S., Li, J. B., Chi, B. and Wen, Z. H., The effect of sintering temperature on porous silica composite strength. *J. Porous Mater*., 2003, **10**, 41–45.
22. Biener, J., Nyce, G. W., Hodge, A. M., Biener, M. M., Hamza, A. V. and Maier, S. A., Nanoporous plasmonic metamaterials. *Adv. Mater*., 2008, **20**, 1211–1217.
23. Cortie, M. B., Maroof, A. I., Stokes, N. and Mortari, A., Mesoporous gold sponge. *Aust. J. Chem*., 2007, **60**, 524–527.
24. Biener, J. *et al.*, Surface-chemistry-driven actuation in nanoporous gold. *Nature Mater*., 2008, **8**, 47–51.
25. Jin, R. H. and Yuan, J. J., Fabrication of silver frameworks using poly(ethyleneimine) hydrogel as a sacrificial template. *J. Mater. Chem*., 2005, **15**, 4513–4517.

ACKNOWLEDGEMENTS. We thank the Department of Science and Technology, New Delhi for providing funds through a research project and a Junior Research fellowship to R.B. We also thank Prof. Stephen Mann, University of Bristol, UK for help.

Received 5 August 2010; revised accepted 23 March 2011

Money handling and obesity: a test of the exaptation hypothesis

Shraddha Karve[1], Ketaki Shurpali[2], Neelesh Dahanukar[1], Sharayu Paranjape[3], Maithili Jog[4], Prajakta Belsare[5] and Milind Watve[1,6,*]

[1]Indian Institute of Science Education and Research, Pune 411 021, India
[2]National Chemical Laboratory, Pune 411 008, India
[3]Department of Statistics, and [5]Department of Zoology, University of Pune, Pune 411 007, India
[4]Department of Biotechnology, Abasaheb Garware College, Karve Road, Pune 411 004, India
[6]Anujeeva Biosciences Pvt Ltd, Pune 411 030, India

The food reward centres in the brain play a central role in the regulation of food intake and thereby obesity. In the modern lifestyle, a number of artificial rewards such as money have been introduced and brain areas evolved for handling food rewards appear to be exapted to handle money and other rewards. This implies that the changing behaviour related to these rewards could influence obesity. Considering money as a reward, we conducted a survey of 211 full-time cashiers to test whether ownership over cash, amount of cash handled and duration of cash-handling work correlated with obesity parameters. Body mass index was significantly affected by sex, ownership, amount of money handled and duration of cash-handling service. Waist-to-hip ratio was significantly affected by sex, amount of money handled and marginally by ownership. The results are compatible with the exaptation hypothesis. It is possible that increasing importance of non-food rewards may play a significant role in the obesity epidemic.

Keywords: Body weight, economics of obesity, exaptation hypothesis, money handling.

OBESITY has become a major health concern worldwide[1]. Since obesity is associated with adverse health outcomes, increased health expenditures and increased risk of numerous co-morbidities[2], efforts are being made to understand the factors that are responsible for the prevalent obesity epidemic. Several genetic, metabolic, socio-economic and behavioural explanations are now available to account for the observed patterns of global increase in obesity. A large number of genes appear to influence body weight[3,4]. However, it is unlikely that the sudden rise in the proportion of obese people in many societies is due to increase in the frequency of any of the genes. A classical metabolic theory suggests that genetic or acquired 'thriftiness' in metabolism is a predisposing factor for obesity[5,6]. However, this view has been challenged

*For correspondence. (e-mail: milind@iiserpune.ac.in)